Reducing ambiguity in fractured-porous media characterization using single-well tracer tests

I. GHERGUT[1], C. McDERMOTT[2], M. SAUTER[1], M. HERFORT[3] & O. KOLDITZ[2]

1 *Applied Geology Group, Geosciences Centre (GZG), University of Göttingen, Goldschmidtstrasse 3, D-37077 Göttingen, Germany*
iulia.ghergut@geo.uni-goettingen.de

2 *Geo-Hydro-Informatics Group, Applied Geosciences Centre (ZAG), University of Tübingen, Sigwartstrasse 10, D-72076 Tübingen, Germany*

3 *Engineering Geology Group, ETH Zurich, Hoenggerberg, CH-8093 Zurich, Switzerland*

Abstract The specific area of the contact surface between fractures and rock matrix, that has an important role in solute and heat transport in fractured-porous reservoirs, is not properly captured by hydraulic and geophysical tests, nor by flow-path tracings in highly dispersive flow fields. A single-well tracing method that increases the sensitivity of tracer breakthrough curves with regard to the contact-surface area parameter is described, with its first application in deep (geothermal) reservoirs in Germany.

Keywords dual-tracer; fractured-porous contact surface; matrix diffusion; push-pull

THE DUAL-TRACER, PUSH-PULL METHOD

The focus of this paper is on assessing contact surfaces in geothermal reservoirs (generally fractured-porous media) by means of tracer tests. Any geothermal energy recovery scheme based on heat transfer from hot rock to circulating fluids essentially depends upon the contact surface between the rock matrix and the open fracture network. The size and geometry of this surface (Fig. 1) cannot unambiguously be determined by hydraulic or geophysical methods, nor from the short-term temperature signals that are usually available. Basically, tracer methods are used either to determine residence times or the *volume* (mobile-domain porosity) of a flow system, or to determine the size of relevant internal *surfaces* within the system in terms of tracer interactions or processes taking place at these surfaces. Yet the application of usual flow-path tracing methods often faces the problem of parameter ambiguity (especially in highly dispersive flow fields), since the same typical effects on "non-conservative" tracer breakthrough curves (BTCs), like retardation, signal damping and long tailings, can be produced by a variety of processes (Carrera *et al.*, 1998), which are not uniquely related to the target contact surface. Hence the need emerged for a special tracing method that reduces the influence of non-surface-related processes upon tracer BTCs, while enhancing the visibility of the effects of matrix diffusion and/or sorption.

The dual-tracer, push-pull method was developed by Sauter (2002) and Herfort & Sauter (2003) as a version of single-well (SW), injection-withdrawal (SWIW) methods. A selection of water-soluble tracers is injected into the reservoir ("push"), and left within it for a certain time during which the tracers can diffuse into the rock

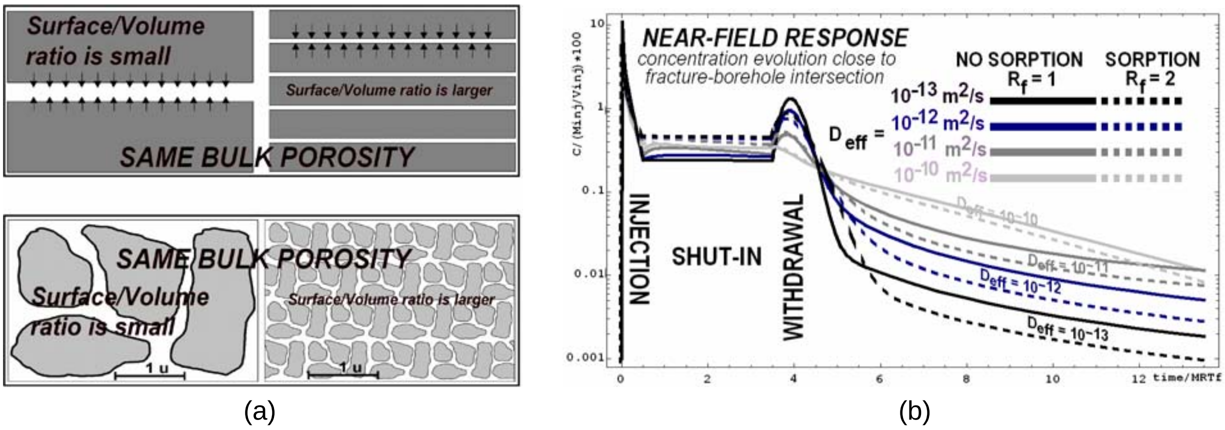

Fig. 1 (a) Specific contact-surface areas (A/V) in a multi-porous or hybrid system. (b) Typical tracer BTCs in a push-pull test; they may reflect borehole size (and mixing) effects at early times.

matrix and undergo further physico-chemical interactions (e.g. sorption) at fracture surfaces or at inner pore walls. Upon withdrawal of the spiked water from the reservoir ("pull"), tracer concentrations will show different signals according to their different ("dual") diffusion/interaction properties (Fig. 1). From the relative difference of measured tracer BTCs, the size of the surfaces at which tracers diffused and/or interacted can be determined. It is this surface-area parameter that the tracer BTCs will be most sensitive to, owing to the SWIW design of the test. Here, "dual" stands for, theoretically at least (and in practice often more than), two tracers with contrasting diffusion and/or sorption properties, which should be ascertained from laboratory experiments.

A single-well (SW) tracing method, consisting of a short tracer injection followed by a free-drift phase, was first designed by Novakowski *et al.* (1998) to investigate fracture transport. Haggerty *et al.* (2000) applied SWIW tracings to test hypothetical distributions of diffusion path lengths in the rock matrix.

Parameter influence and sensitivity issues

The specific area (i.e. area per bulk volume) σ of the contact surface between the adjacent void-space continua of the hybrid (fractured-porous) system is equivalent to the effective size $L_m = (1 - n_f)\,\sigma^{-1}$ of matrix blocks (with n_f denoting fracture porosity), or to the fracture density, taken as the number of fractures per unit depth of the (local) flow cross-section. An adequate description of matrix diffusion and of further processes at fracture and matrix inner surfaces can depend upon the size and shape of matrix blocks (Carrera *et al.*, 1998; Haggerty *et al.*, 2000). At early as well as very late times, however, tracer BTCs are independent of matrix block shapes. At very early tailing times, the effect of diffusion into (infinite-sized) matrix blocks is also independent of matrix block size. At mid-early tailing times, the effective size of matrix blocks L_m is perceived in terms of two independent parameters expressing the time scale of matrix diffusion/sorption and the strength of advection–diffusion coupling; for instance $\{R_m L_m^2 D_m^{-1}, n_m D_m L_m^{-2}\}$, modulated by some numerical factors characterizing matrix block geometry. For tracer BTC interpretation with imperfectly known diffusion and sorption properties, it is of advantage that L_m (or σ) multiplies different rock and tracer parameters (the physical size of rock matrix blocks is thus not easily "re-scaled", other than by the diffusion coefficient, D_m). Knowing the matrix porosity n_m, effective tracer diffusion coefficients D_m and tracer retardation factors R_f, R_m, for equilibrium processes at outer and inner matrix surfaces, and with fracture porosity n_f assessed from hydraulic or geomechanical tests, one can determine the specific contact-surface area σ from artificial tracer BTCs, if the experiment duration is long enough for BTCs to show their "mid-late" tailings. Unlike traditional flow-path tracings, such tests do not aim to determine a residence time distribution that would characterize a given flow regime in the fracture system, since the very test principle presupposes negligible background flow, and the system volume "seen" by the injected tracer is determined (mainly) by the flushing (chaser) volume. Tracer separation by diffusion/sorption coefficients reverts monotonicity upon transition from peak to tailing phases (Fig. 1); it is advisable to use the latter in fitting the surface-area parameter. At mid-late tailing times, if advection–dispersion effects become negligible, the surface-area estimation reduces to fitting σ to the simple integral equation for the concentration's first derivative:

$$f(t) = \frac{\sigma^2 \phi_m D_m}{R_f \phi_f (1-\phi_f)^2} \int_0^t g(\tau) f(t-\tau)\,\mathrm{d}\tau \tag{1}$$

$$g(\tau) \approx -\frac{2}{\pi^2}\Gamma\left(1; \frac{1}{2} + N_{trune}\right)\delta\left(\frac{\sigma^2 D_m}{R_m (1-\phi_f)^2}\tau\right) - \sum_{n=1}^{N_{Trune}} a_n \exp\left(-\frac{\alpha_n^2 \sigma^2 D_m}{R_m (1-\phi_f)^2}\tau\right) \tag{2}$$

with numerical coefficients a_n and α_n in the approximation for $g(\tau)$ reflecting the geometry and size of the matrix blocks. The derivation of an exact kernel $g(\tau)$ for one clearly specified matrix block geometry, and two alternative ways of approximating $g(\tau)$ (one of which is compatible with multiple matrix block geometries) are described in Carrera *et al.* (1998), while Haggerty *et al.* (2000) postulate several possible forms for $g(\tau)$ within a more general model of multi-rate exchange between mobile and immobile zones, yielding characteristic BTC tailing patterns. This latter approach is not followed here, because the duration of the tests conducted (cf. Table 1, second part) was too short. The presuppositions for applying equation (1) are not fully met by the tests listed in Table 1, but even in this case one may use expression (2) to uncouple the source/sink term created by matrix diffusion in the transport equations at time t from fracture solute concentration values at all times $t' < t$, thus yielding (after spatially discretizing the mobile zone and without needing to discretize the immobile zone) a system of first-order ordinary differential eqations (ODEs) with regard to time (with domesticated initial values), which can be solved by the method of lines, using, for instance, *Mathematica*'s ODE solver.

FIRST EXPERIENCES WITH THE DUAL-TRACER PUSH-PULL METHOD IN GERMANY

Several single well (SW) tests conducted within a comprehensive geothermal reservoir tracing programme, started in 2003, are outlined in Table 1. Tests #5,6 are not of the

Table 1 Overview of tracer tests discussed in this paper.

#	Site and borehole identification	Site location and characteristics	Type of test; system size	Target information
1	"Lindau" underground facility for fractured rock testing, borehole N8	Black Forest, shallow granite formation (crystalline rock), hydrothermally altered, highly-permeable fault zone	SW, push-pull, <20 m^3	contact-surface area (fracture density) (>100 $m^2\,m^{-3}$)
2	Urach Spa, borehole Urach-3 (pilot geo-thermal project)	Swabian Alb, crystalline basement, 4.4 km deep (< ~170°C), "hot-dry rock" type, low permeability, several fracture systems in 3–4 km depth	SW, push-pull, <1500 m^3	contact-surface area (<3 $m^2\,m^{-3}$)
3	KTB ("Kontinentale Tiefbohrung"), pilot borehole, before hy-draulic stimulation	NE Bavaria, crystalline basement, 4 km depth (~120°C), good permeability (KTB is the German site of the Int. Continental Drilling Programme)	SW, push-pull, <1000 m^3 (within <<-scale fault system)	contact-surface area before hydraulic stimulation (10–30 $m^2\,m^{-3}$)
4	KTB, pilot borehole, after massive hydrau-lic stimulation	*ibid.*, 4 km depth (cooling to ~50°C estimated), enhanced permeability, fracture network structure may be changed by coupled THM processes	SW, push-pull, <10 000 m^3 (within larger-scale fault sys.)	contact-surface area after hydraulic stimulation; cooling effects
5	KTB, pilot borehole and main borehole, during and after *ibid.*	*ibid.*, suspected transport connection between fracture systems in 5 and 7 km depth (~210°C), within complex conti-nental fault system	monopole-to-monopole (broken dipole), flow-path tracing, >10^5 m^3	transport-effective porosity, contact-surface area, fault structure
6	Horstberg, borehole Z1 (using inner/outer casing as "2 boreholes in 1")	Lower Saxony, sedimentary basin, two sandstone horizons at ~3.6 and ~3.8 km depth (~150°C), connected by hydrofrac (created by massive water injection just before adding tracer)	SW, monopole (divergent), flow-path tracing; esti-mated reservoir void-space > 10^4 m^3	transport properties of hydrofrac, contact-surface area ($10^{3\text{-}4}$ $m^2\,m^{-3}$), contact time within upper horizon

Table 1 continued ($V_{B,in,out}$ denote the borehole, the injected, and the extracted volumes).

#	Drawbacks with test design, and failures in test execution	Models and methods used
1	Packer failure, borehole not properly flushed (despite V_{in} / V_B ~ 5, and despite having adjusted the density of injected solution to match formation fluid density; V_{out} / V_{in} ~ 10 still insufficient)	Advection–dispersion in parallel-plate multiple-fracture system (1-D), matrix diffusion (1-D), equilibrium or first-order kinetic sorption at fracture surfaces and within rock matrix, mid-late BTC approximations, F–C diagram in flow-path tracings, "transfer–storage" diagram in push-pull tests; parameters assumed as known: – fracture porosities (except for #5,6); – matrix porosities; – tracer diffusion coefficients (calculated from matrix poro-sities, formation temperatures, and corresponding fluid viscosities; salinity influences not quantified as yet).
2	V_{in} / V_B ~ 1.5 ; V_{out} / V_{in} ~ 3.2 ; undifferentiated injection of same tra-cers simultaneously into at least 2 different fracture systems; at least one tracer not fully dissolved before injection (tracer mass actually entering target system remains unknown → BTCs cannot be normalized, and BTCs' height difference cannot be interpreted)	
3	V_{in} / V_B ~ 2.6 ; V_{out} / V_{in} ~ 2.4 (both rather low)	
4	V_{in} / V_B ~ 2.6 ; V_{out} / V_{in} ~ 4.2 (both rather low)	
5	Test design imposed by project financing structure: first radially diver-gent flow from pilot hole, next >1 year resting, then radially convergent flow to main hole → unnecessarily high dilution of tracers in the for-mation (requiring injection of large tracer quantities, which prohibits the use of "chemically inert" tracers like HTO), and long in-situ residence times (→ increased risk of tracer loss by thermal decay); V_{in} / V_B was large enough, but V_{out} / V_{in} is likely to be insufficient	
6	V_{in} / V_B ~ 14 sufficient, but V_{out} / V_{in} ~ 2.8; divergent flow field → high tracer dilution; extreme salinity of formation fluid raises detection limits and reduces detection accuracy for all tracers (including tritium)	

push-pull type, but provide some elements for comparison. Tracer BTCs from test #3 are shown in Fig. 2. Note that tests #3,4 were conducted in the same formation but in quite different thermo-hydro-mechanical state: test #3 in a depleted system, during

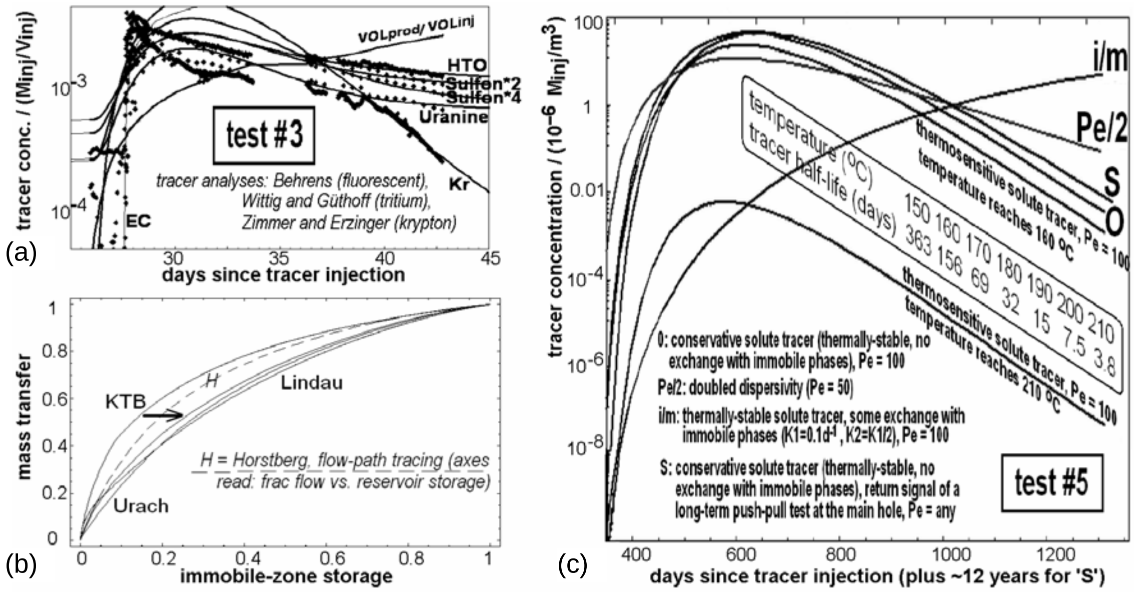

Fig. 2 (a) Tracer BTCs from test #3, with mid-late fit of transformed model. (b) Comparison of "F–C" diagrams for the four test sites named in Table 1; arrow indicates change in KTB reservoir structure after massive hydraulic stimulation. (c) Tracer fate and BTC expectation spectrum at the main KTB hole as of 2007 (test #5): half-life values assumed for the unnamed "thermosensitive tracer" are hypothetical—they were calculated from a two-parameter Arrhenius-type formula with values chosen such as to produce half-lives in the range of those measured for uranine (in the presence of different rock minerals, however) by Adams & Davis (1991) and Rose *et al.* (2001).

the recovery phase following a long-term pumping test; test #4 in a relaxing over-pressurized system, following a long-term stimulation (injected cold water >> previously abstracted fluid volume); coupled THM processes (e.g. cooling-induced cracks), were expected to raise σ (among other effects). The tracer slug for test #5—meant as a flow-path tracing between the two KTB (Kontinentale Tiefbohrung, Continental Deepwell Drilling) boreholes—had to be added during the massive water injection and thus it preceded the tracer slug for test #4 (push-pull type); thereby slug #5 also generates a push–pull signal during the withdrawal phase of test #4, super-imposing the push–pull signal from slug #4. To facilitate BTCs separation, slug #4 was moderately oversized (with regard to target formation size). Slug #3, of which some 50% (cf. Table 2) had been left inside the formation before the start of massive stimulation, was no longer expected to produce detectable signals during tests #4,5. Separation of BTCs stemming from tracer slugs #4 and #5 was based on closed-form approximations for early (#5) and mid-late (#4) times; push–pull signals from slug #5, of which only an incipient ascending phase can be captured by free outflow at the injection hole, characterize a much larger formation volume and they become increasingly univoque as the tailings from slug #4 gradually vanish. At the elevated formation temperatures encountered in all tests except #1, tracer sorption is supposed to be negligible; for test #1, assumptions on sorptivity can be inferred from Behrens (1986). All tracers used (listed in Table 2) can be regarded as approximately thermally-stable for the duration of the respective test, except for test #5 in which thermal decay may lead to considerable tracer loss (cf. Fig. 2). The idea of test #5 is explained in some

Table 2 Tracers used in field tests (numbered as in Table 1); tracer recoveries against fluid outflow.

#	Actual fluid production (approximate field records)	BTCs extrapolated to	Tracers[a] used and tracer recovery values (actual, extrapolated)[b]	
1	Free outflow: 1500 L in 3 h (stopped)	17 h (assuming exponential decrease of outflow rate)	Uranine NDS Naphthionate Lithium Bromide	(3.8% , 7%) (4.9% , 9.1%) (3.1% , 5.5%) (3.4% , 6.1%) (4.3% , 8.2%)
2	Free outflow (regulated): 438 m^3 in 5 days (stopped)	100 days (assuming exponential decrease of outflow rate)	Uranine NDS freshwater tracers	(53% , 72%) (60% , 82%) (no data as yet)
3	Forced outflow (pumping): 300 m^3 in 16 days (stopped)	100 days (assuming constant pumping rate)	Uranine NDS PTS HTO	(38% , 51%) (54% , 85%) (54% , 89%) (50% , 86%)
4	Free outflow: 520 m^3 in 6 days (ongoing)	100 days (assuming exponential decrease of outflow rate)	Uranine NDS HTO	(28% , 30%) (36% , 44%) (24% , 32%)
5	(Shut-in phase till 2007, then forced outflow, about 22×10^3 m^3 planned)	(up to 10^4 days might be necessary)	Uranine NDS freshwater tracers	(<0.5% to date)[c] (<0.5% to date)[c] (no data as yet)
6	Free outflow: 3600 m^3 in 10 days (stopped)	100 days (assuming exponential decrease of outflow rate)	Uranine NDS HTO	(6.4% , 8%) (10% , 12.4%) (7.4% , 10.3%)

[a] "Uranine" is a common name for disodium fluorescein; "NDS" abbreviates 1,5-naphthalene disulfonate (disodium salt); "PTS" abbreviates 1,3,6,8-pyrene tetrasulfonate (tetrasodium salt), a special water tracer synthetized by H. Behrens (Munich, 1980) and kindly offered for use in this test, whose remarkably "conservative tracer" properties in several types of soil and rock are described in Netter & Behrens (1992) and Machate *et al.* (1998); "HTO" abbreviates tritiated water (note: even this tracer is not fully chemically-inert, in that the degree of hydratization of water molecules themselves—determining effective molecule sizes and thus diffusion coefficients—is influenced by the salinity of formation fluids, which is not negligible in tests #2,5,6);

[b] Estimated, with the reservation that available outflow data and tracer analyses are not final;

[c] Estimations pertain to push-pull signals induced by slug#5 at its injection hole.

detail here: the massive hydraulic stimulation conducted at the pilot KTB hole, with about 84×10^3 m^3 of cold freshwater injected between mid 2004 and mid 2005, has provided the opportunity for probing a solute transport connection between the two seismic reflectors intersected by the main, 9-km deep KTB hole (of which only the upper is intersected by the pilot, 4-km deep KTB hole), given the prospect of a long-term abstraction to start at the main hole by mid 2007. To appreciate the chance of a pilot-hole injected tracer re-appearing at the main hole in due course and to assist in dimensioning tracer slug #5 (added before the last 16×10^3 m^3 of injected freshwater), a number of transport scenarios were simulated (Fig. 2) within a simplified 2-D model of reflector zone projections, using transport parameter estimations from the first push–pull test (#3) at this site, and assuming an average fracture porosity of 5×10^{-5} (estimated from hydraulic testing at the injection (pilot) hole by McDermott & Kolditz, 2004). Tracer quantities in slug #5 were limited by legal/environmental considerations; as a consequence, if the effective fracture porosity n_f of the assumed transport connection exceeds 2×10^{-4} (estimated from hydraulic testing at the extraction (main) hole by Kessels *et al.*, 2004), tracer concentrations at the main hole may stay below detection limits for the whole duration of the planned fluid abstraction as of 2007—note: fracture porosity n_f is not a scaling parameter of the complete transport problem, not even for a conservative tracer, thus a $N\times$ higher n_f is not compensated just by injecting the N-fold tracer quantity. Additionally, the withdrawal signal (curve “S” on Fig. 2) of a long-term “push–pull” hypothetically and involuntarily performed by drilling fluids in the main hole can characterize fracture surfaces around the main hole (not the flow connection between the two boreholes), but it may also interfere with the analytics of (purportedly injected) fluorescent tracers.

In order to estimate the surface-area parameter σ, a simplified model formulated such as to yield the same mid-late behaviour of BTCs was fitted to the latest segment of measured BTCs from each test. Plotting the zeroth-order temporal moment *versus* the first-order temporal moment of BTCs truncated to time t (with t running from 0 to “practical infinity”, and with both moment ranges rescaled by their last computed value) yields a dimensionless characterization for the fractured-porous reservoir, useful for comparison purposes (Fig. 2), with the advantage of being invariant to hydraulic variables (as long as the flow regime does not change qualitatively), and insensitive to tracer BTC calibration errors or uncertainties (which may stem from tracer analytics, or from the impossibility of estimating the tracer mass actually entering the target system, cf. test #2 in Table 1, second part). Some authors interpret the resulting diagram as a “geometric characterization” (Shook, 2003) of the reservoir. If derived from a flow-path tracing, this normalized $M_0(t)$ *versus* $M_1(t)$ diagram is indeed analogous to the FC (flow–capacity) diagrams commonly used in fissured/fractured media hydraulics. When derived from a push–pull tracing, the diagram’s meaning is to correlate mass transfer (recovery) with contact time, and its analogy to a FC diagram is less intuitive. In order to calculate the temporal moments, the measured BTCs need to be extrapolated for large times according to some transport model (the choice of a particular matrix block geometry has in fact little influence upon the computed moments); most representative of fluid flow/storage is the diagram derived from the BTC of the “most conservative” and least diffusive tracer used in each test (this was taken to be PTS for test #3, and NDS for the other tests, cf. Table 2).

CONCLUDING REMARKS

The power of the dual-tracer push–pull method lies in its enhanced parameter sensitivity with regard to contact-surface areas, but the determination of contact-surface areas from tracer BTCs presupposes reliable knowledge of tracer properties. A tentative interpretation of BTC height differences between different tracers, beyond the amount accountable for by their different diffusion coefficients, can first rely on structure-activity considerations (Behrens, 1986), before tracer thermostability and sorption are quantified in laboratory experiments; a field push–pull test can substitute the required laboratory investigations if at least one assuredly “reference” tracer is injected alongside with the tracers whose physico-chemical behaviour is less secured. In the practice of deep reservoir tracing, there are physical limitations to test design, and financial limitations to test duration. Insufficient flushing volumes render BTC peak regions unusable for fracture characterization, and insufficient outflow volumes (durations) make characteristic “mid-late” BTC slopes difficult to recognize. In the examples of single-well tracing tests provided here, however, specific contact surfaces could be estimated and an overall system characterization was possible at least for comparative purposes, despite the volume and duration design of the tests considerably deviating from the principle recommendations as these would result from parameter sensitivity analyses.

Acknowledgements Financial support from the German Research Foundation (DFG, project Sa-501/16/1-4), from the Stadtwerke Bad Urach, the GGA Hannover and the GFZ Potsdam is gratefully acknowledged. Expert tracer knowledge provided by H. Behrens (Germany) was essential to both the design and the interpretation of all tests. Field work in tests #2, #3, and #4 was led by M. Lodemann (University of Göttingen).

REFERENCES

Adams, M. C. & Davis, J. (1991) Kinetics of fluorescein decay and its application as a geothermal tracer. *Geothermics* **20**(1/2), 53–66.

Behrens, H. (1986) Water tracer chemistry—a factor determining performance and analytics of tracers. In: *Symposium on Underground Water Tracing* (ed. by A. Morfis & P. Paraskevopoulou) (Proc. 5th Int. Symp. SUWT, Athens, Greece), 121–133.

Carrera, J., Sánchez-Vila, X., Benet, I., Medina, A., Galarza, G. & Guimera, J. (1998) On matrix diffusion: formulations, solution methods and qualitative effects. *Hydrogeol. J.* **6**, 178–190.

Haggerty, R., McKenna, S. A. & Meigs, L. C. (2000) On the late-time behavior of tracer test breakthrough curves. *Water Resour. Res.* **36**(12), 3467–3479.

Herfort, M. & Sauter, M. (2003) Investigation of matrix diffusion in deep hot-dry-rock reservoirs using SWIW tracer tests. In: *Groundwater in Fractured Rocks* (ed. by J. Krasny, Z. Hrkal & J. Bruthans) (Proc. Int. Conf. GWFR’2003, September 2003, Prague, Czech Republic), 257–258.

Kessels, W., Kaiser, R. & Graesle, W. (2004) Hydraulic test interpretation with pressure dependent permeability – Results from the continental deep crystalline drilling in Germany. In: *2nd Int. Symp. on Dynamics of Fluids in Fractured Rock* (Berkeley, California, USA).

Machate, T., Behrens, H., Klotz, D., Noll, H., Schramm, K. W. & Kettrup, A. (1998) Evaluation of hydraulic characteristics and flow pattern in a CWTP by means of tracer studies: Part I, II. *Freshwater Environ. Bull.* **7**, 635–647.

McDermott, C. I. & Kolditz, O. (2004) Hydraulic-geomechanical effective stress model: determination of some discrete fracture network parameters from a pump test and application to geothermal reservoir modelling. In: *29th Workshop on Geothermal Reservoir Engineering* (Stanford University, California, USA).

Netter, R. & Behrens, H. (1992) Application of different water tracers for investigation of constructed wetland hydraulics. In: *Tracer Hydrology* (ed. by H. Hötzl & A. Werner), 125–129. Balkema, Rotterdam, The Netherlands.

Novakowski, K. S., Lapcevic, P. A., Voralek, J. W. & Sudicky, E. A. (1998) A note on a method for measuring the transport properties of a formation using a single well. *Water Resour. Res.* **34**(5), 1351–1356.

Rose, P. E., Benoit, W. R. & Kilbourn, P. M. (2001) The application of the polyaromatic sulfonates as tracers in geothermal reservoirs. *Geothermics* **30**(6), 617–640.

Sauter, M. (2002) Hot-Dry-Rock Bad Urach. Tracer experiments in borehole Urach 3. *Task Paper 2/02, Univ. Göttingen, Germany*.

Shook, G. M. (2003) A simple, fast method of estimating fractured reservoir geometry from tracer tests. *Geothermal Research Council Transactions* **26**.